The EMBO Journal Vol. 22 No. 15 pp. 3930–3940, 2003

Efficient RNA 2′-*O*-methylation requires juxtaposed and symmetrically assembled archaeal box C/D and C′/D′ RNPs

Elizabeth J.Tran, Xinxin Zhang and E.Stuart Maxwell[1]

Department of Molecular and Structural Biochemistry, North Carolina State University, Raleigh, NC 27695-7622, USA

[1]Corresponding author
e-mail: stu_maxwell@ncsu.edu

Box C/D ribonucleoprotein (RNP) complexes direct the nucleotide-specific 2′-*O*-methylation of ribonucleotide sugars in target RNAs. *In vitro* assembly of an archaeal box C/D sRNP using recombinant core proteins L7, Nop56/58 and fibrillarin has yielded an RNA:protein enzyme that guides methylation from both the terminal box C/D core and internal C′/D′ RNP complexes. Reconstitution of sRNP complexes containing only box C/D or C′/D′ motifs has demonstrated that the terminal box C/D RNP is the minimal methylation-competent particle. However, efficient ribonucleotide 2′-*O*-methylation requires that both the box C/D and C′/D′ RNPs function within the full-length sRNA molecule. In contrast to the eukaryotic snoRNP complex, where the core proteins are distributed asymmetrically on the box C/D and C′/D′ motifs, all three archaeal core proteins bind both motifs symmetrically. This difference in core protein distribution is a result of altered RNA-binding capabilities of the archaeal and eukaryotic core protein homologs. Thus, evolution of the box C/D nucleotide modification complex has resulted in structurally distinct archaeal and eukaryotic RNP particles.

Keywords: Archaea/box C/D RNP/ribonucleotide methylation/snoRNA/sRNA

Introduction

The small nucleolar RNAs (snoRNAs) play critical roles in ribosome biogenesis, functioning in the processing and modification of preribosomal RNA (Bachellerie *et al*., 2002; Kiss, 2002; Terns and Terns, 2002). The primary role of the vast majority of snoRNAs is to guide the site-specific modification of rRNA nucleotides. Guide regions within the snoRNA base pair with complementary sequences in the rRNA and direct snoRNA-associated enzymes to the designate nucleotide for ribose or base modification. Recent work has also revealed guide RNAs in Archaea (Gaspin *et al*., 2000; Omer *et al*., 2000). While archaeal organisms do not possess a nucleus, they nevertheless utilize snoRNA-like RNAs (sRNAs) for nucleotide modification. The occurrence of guide RNAs in both Eukarya and Archaea indicates that the process of RNA-guided nucleotide modification is an ancient mechanism predating the divergence of Eukarya and Archaea more than 2 billion years ago.

Box C/D RNAs direct the site-specific 2′-*O*-ribose methylation of targeted nucleotides within rRNA and other RNA substrates (Tollervey, 1996; Tycowski *et al*., 1998; Jady and Kiss, 2001). Members of this family are defined by the conserved boxes C and D located at the 5′ and 3′ termini, respectively (Tyc and Steitz, 1989; Caffarelli *et al*., 1996; Cavaille and Bachellerie, 1996; Watkins *et al*., 1996, 2000). These conserved sequences fold into a stem–loop–stem structure which is essential for the binding of box C/D ribonucleoproteins (RNPs) as well as the nucleotide modification reaction itself. Additional internal sequences designated C′ and D′ boxes can be identified in eukaryotic snoRNAs and archaeal sRNAs (Kiss-Laszlo *et al*., 1998). Although based upon boxes C and D, the C′ and D′ sequences are not as strictly conserved and are not easily identified in all eukaryotic snoRNAs. However, both RNA motifs guide 2′-*O*-methylation of targeted ribonucleotides using rRNA-complementary regions located immediately upstream of boxes D and D′. Antisense sequences 10–21 nucleotides in length base pair with the target RNA and direct methylation to the designate nucleotide positioned five nucleotides upstream of box D/D′ within the snoRNA:rRNA duplex (Cavaille and Bachellerie, 1998).

Eukaryotic box C/D snoRNAs associate with four core proteins: the 15.5 kDa protein, nucleolar protein 56 (Nop56p), nucleolar protein 58 (Nop58p) and fibrillarin. Assembly of the terminal box C/D snoRNP complex is required for snoRNA processing and stable accumulation of the box C/D snoRNAs (Caffarelli *et al*., 1996; Cavaille and Bachellerie, 1996; Watkins *et al*., 1996). The 15.5 kDa protein binds the terminal box C/D core motif in the absence of the other core proteins and initiates snoRNP assembly (Watkins *et al*., 2000). Nop56p and Nop58p are highly related snoRNP core proteins also required for ribosome biogenesis (Lafontaine and Tollervey, 1999, 2000; Newman *et al*., 2000). Fibrillarin is the fourth core protein and all available biochemical and genetic evidence indicates that it is the methylase enzyme (Tollervey *et al*., 1993; Wang *et al*., 2000; Galardi *et al*., 2002; Omer *et al*., 2002). Recent work has revealed the asymmetric distribution of the box C/D snoRNP core proteins upon the terminal box C/D core and internal C′/D′ motifs (Cahill *et al*., 2002; Szewczak *et al*., 2002). Based upon nucleotide modification experiments, the 15.5 kDa core protein binds exclusively to the terminal box C/D core motif. *In vivo* crosslinking revealed that core proteins Nop58 and Nop56 are differentially bound to the box C/D and C′/D′ motifs, respectively. Only fibrillarin, the putative methylase, is a component of both the box C/D and C′/D′ RNP complexes.

Archaeal box C/D sRNP complexes exhibit a distinctly different protein composition from that of eukaryotic box C/D snoRNPs. Only three core proteins are required

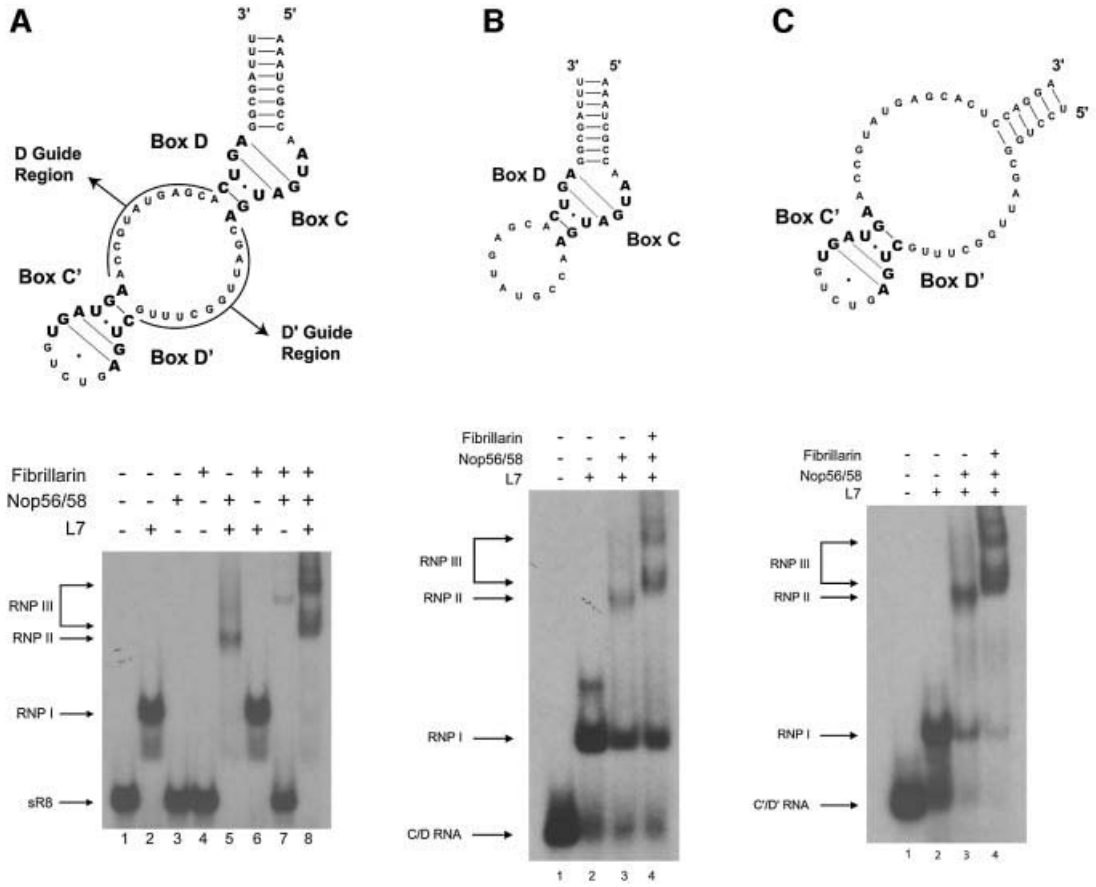

Fig. 1. Archaeal sR8 sRNP assembly requires a defined order of core protein addition and forms symmetric RNP complexes on the terminal box C/D core and internal C′/D′ motifs. (**A**) The folded structure of *M.jannaschii* sR8 sRNA with terminal box C/D core and internal C′/D′ motifs is based upon the consensus structure of the snoRNA box C/D motif implied from the crystal structure of the15.5 kDa binding site on the U4 snRNA (Vidovic *et al*., 2000; Watkins *et al*., 2000). Lower panel: sR8 sRNP complexes were assembled by incubating L7, Nop56/58 and fibrillarin core proteins, either individually or in different combinations, with 5′-radiolabeled sR8 sRNA. Assembled complexes were resolved on 4% native polyacrylamide gels and RNPs were visualized by autoradiography. Migration positions of the partially assembled (RNP I and RNP II) and complete (RNP III) RNP complexes are indicated. (**B** and **C**) The terminal box C/D core and internal C′/D′ RNA half-molecules are derived from the wild-type sR8 full-length sRNA. Lower panels: terminal box C/D core and internal C′/D′ RNPs were assembled by incubating 5′-radiolabeled RNA with the indicated sRNP core proteins. Migration positions of the partial (RNP I and RNP II) and fully assembled RNPs (RNP III) are indicated. The slower migrating complex in lane 2 of (C) is non-specific L7 binding to the RNA at elevated L7 concentrations.

for sRNP assembly. Ribosomal protein L7 functions as the archaeal homolog of 15.5 kDa protein and a single archaeal Nop56/58 protein takes the place of the eukaryotic Nop56p/Nop58p protein pair (Kuhn *et al*., 2002; Omer *et al*., 2002; Tang *et al*., 2002). An archaeal homolog of fibrillarin which exhibits high homology with its eukaryotic counterpart is the third archaeal sRNP core protein (Amiri, 1994), and its crystal structure has revealed an *S*-adenosyl methionine-binding site, consistent with its role as the methylase enzyme (Wang *et al*., 2000). Recently, a *Sulfolobus acidocaldarius* box C/D sRNP complex has been assembled *in vitro* using recombinant core proteins (Omer *et al*., 2002). This complex was shown to direct 2′-*O*-methylation from its terminal box C/D core motif.

In the work reported here, we have reconstituted a methylation-competent *Methanococcus jannaschii* box C/D sRNP complex which guides methylation from both the terminal box C/D core and internal C′/D′ RNA motifs. Strikingly, we demonstrate that efficient methylation requires that the terminal box C/D and internal C′/D′ RNP complexes function within the full-length sRNA molecule. RNA:protein binding studies also revealed that the internal C′/D′ motif is distinct in structure from the terminal box C/D core motif. In contrast to the asymmetric eukaryotic snoRNP, the archaeal sRNP complex is symmetric and requires all three core proteins for RNP assembly on the box C/D core and internal C′/D′ motifs. Comparative protein binding studies demonstrated the different RNA-binding capabilities of the L7 and 15.5 kDa protein homologs on the box C/D and C′/D′ motifs. These studies now provide a biochemical rationale for the symmetric versus asymmetric RNP structure of the archaeal and eukaryotic box C/D RNPs, respectively.

Results

sRNP core proteins L7, Nop56/58 and fibrillarin bind both the terminal box C/D core and internal C′/D′ motif to assemble symmetric RNP complexes

Methanococcus jannaschii sR8 was selected as the model sRNA for *in vitro* sRNP assembly. Figure 1A (upper

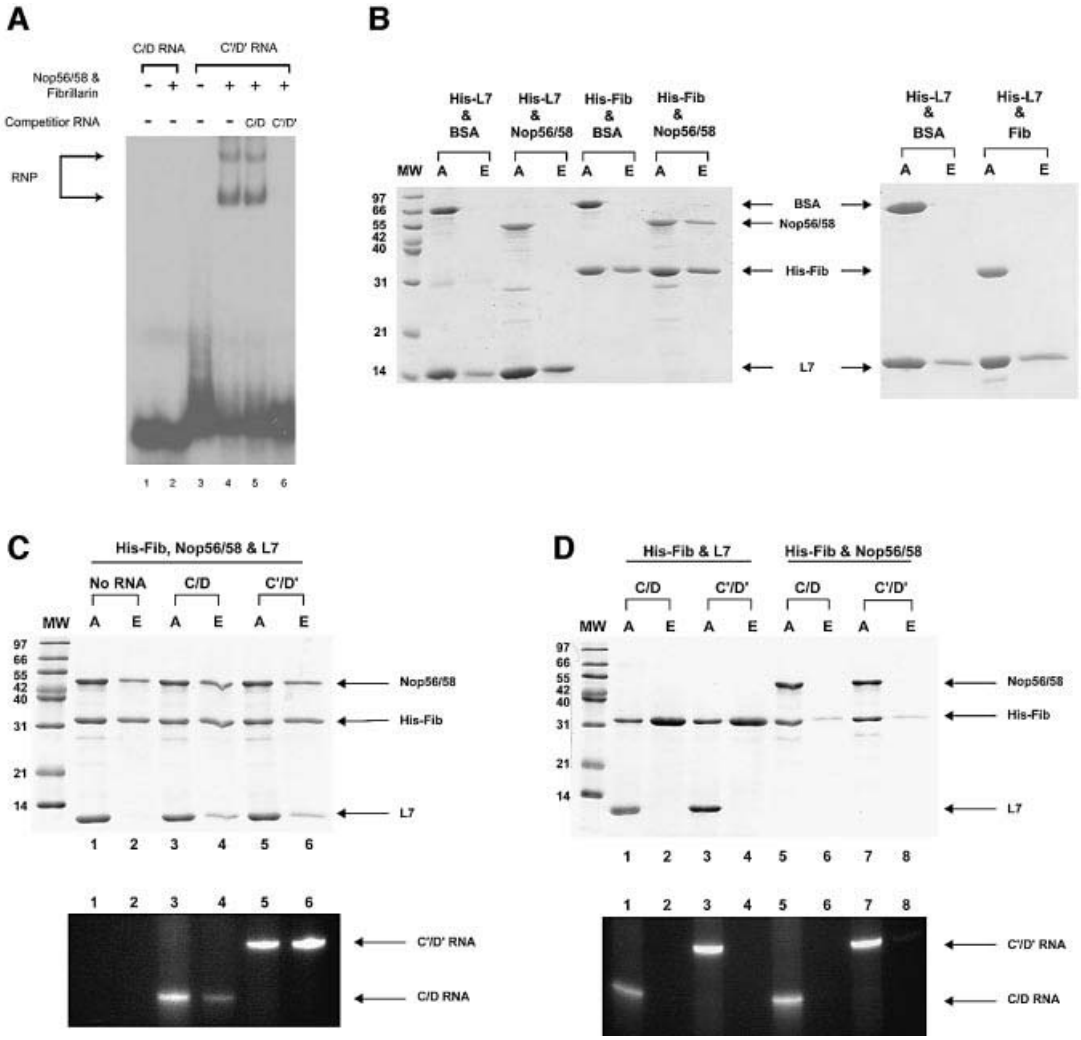

Fig. 2. Nop56/58 and fibrillarin interact via protein–protein interactions and can bind the internal C′/D′ motif in the absence of core protein L7. (**A**) Nop56/58 and fibrillarin core proteins bind specifically to the C′/D′ motif in the absence of L7 core protein. Nop56/58 and fibrillarin were incubated with radiolabeled box C/D or C′/D′ RNA. Assembled RNP complexes were resolved on a native polyacrylamide gel and visualized by autoradiography. Competition experiments included a 1000-fold molar excess of non-radiolabeled box C/D or C′/D′ RNA. (**B**) Nop56/58 interacts with fibrillarin. sRNP core proteins were incubated in equimolar concentrations. Twenty percent of the protein mixture was removed as the applied sample (A) and the remainder applied to affinity resin. Bound proteins were eluted (E), resolved on 14% SDS–polyacrylamide gels and visualized by Coomassie Blue staining. Incubated protein combinations are indicated above each gel lane. (**C** and **D**) Pulldown analysis demonstrates the presence of L7 in the C′/D′ RNP complex. His-tagged fibrillarin, Nop56/58 and L7 were incubated with the C/D and C′/D′ RNAs in various combinations as indicated and fibrillarin was affinity-selected via the His tag. Co-isolated sRNP core proteins (upper panels of C and D) and RNAs (lower panels of C and D) were resolved on polyacrylamide gels and visualized by Coomassie Blue and EtBr staining, respectively.

panel) shows the predicted secondary structure of sR8 with its terminal box C/D core motif and internal box C′/D′ motif. The sR8 sRNP complex was assembled *in vitro* by incubating radiolabeled sR8 sRNA with recombinant *M.jannaschii* sRNP core proteins L7, Nop56/58 and fibrillarin (Figure 1A, lower panel). sRNP assembly exhibited an ordered addition of core proteins with L7 binding first, followed by Nop56/58 and fibrillarin. RNP assembly also required elevated temperatures around 70°C (data not shown). Both the required order of protein binding and the elevated temperature for assembly are consistent with recent observations reported for *in vitro* assembly of an *S.acidocaldarius* box C/D sRNP complex (Omer *et al*., 2002). We suspect that the elevated temperature induces conformational changes in the core proteins and/or the sRNA that are critical for protein binding.

Addition of all three core proteins assembled several large complexes (designated RNP III, lane 8). We do not know the distinct composition of each larger RNP but believe that incomplete assembly upon one or both RNA motifs or alternative conformations of the assembled sR8 RNP generates the multiple complexes. Addition of Nop56/58 to the L7:sR8 RNP complex resulted in the formation of only modest amounts of higher-order RNP II (lane 5). In contrast, addition of both Nop56/58 and fibrillarin resulted in assembly of RNP III complexes in greater amounts. We believe that Nop56/58 and fibrillarin bind the L7:sR8 RNP as a dimer despite the fact that Nop56/58 alone exhibits some binding activity. The highly charged nature of Nop56/58 when it is not complexed with fibrillarin causes significant aggregation of the L7:sR8 RNP (our unpublished results) and the resultant loss of soluble RNP complex (lane 5).

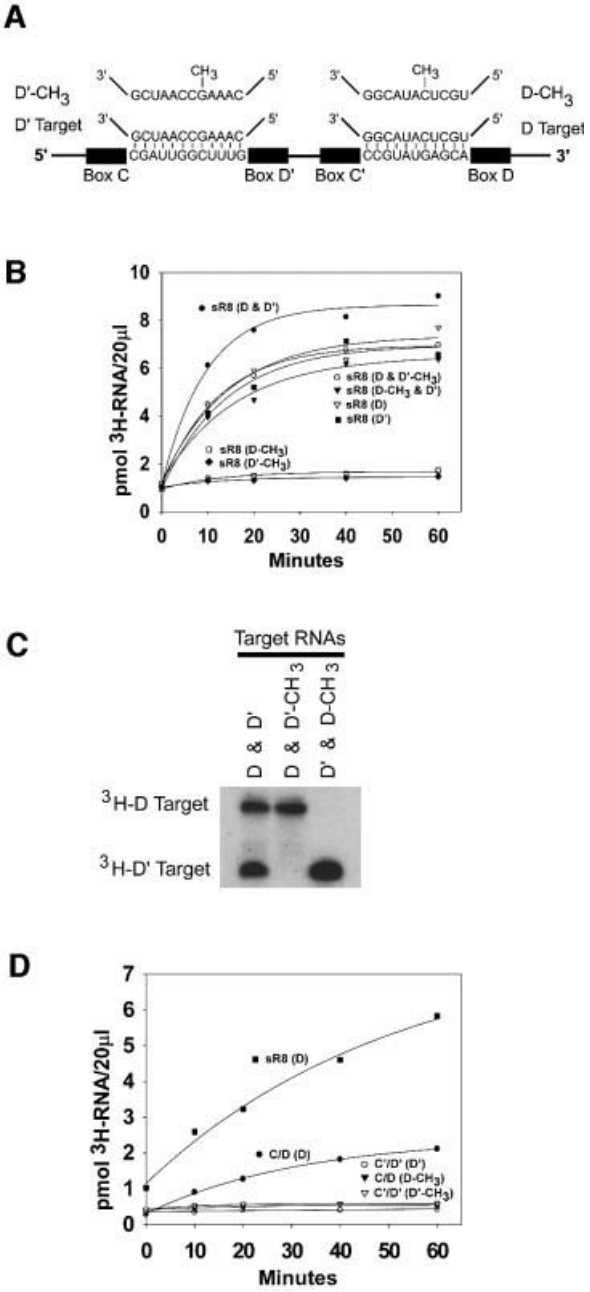

Fig. 3. *In vitro* assembled sR8 sRNP guides site-specific 2′-*O*-methylation from both terminal box C/D and internal C′/D′ RNPs. Efficient methylation requires juxtapositioning of both RNP complexes in the full-length sRNA. (**A**) Schematic presentation of *M.jannaschii* sR8 base paired with D and D′ target RNAs. D-CH_3 and D′-CH_3 target RNAs possessing a previously 2′-*O*-methylated sugar at the designate nucleotide are illustrated above. (**B**) The assembled sR8 sRNP complex guides site-specific methylation of both the D and D′ target RNAs. Assembled sR8 sRNP was incubated at 70°C with the indicated target RNAs (in parentheses) and [^{3}H]SAM. At various times, aliquots of the reaction were collected and TCA precipitated, and [^{3}H]methyl incorporation was measured by scintillation counting. (**C**) Methylation of D and D′ RNA substrates demonstrates site-specific 2′-*O*-methylation at designate nucleotides of the target RNAs. Target RNAs in various combinations indicated above the gel were resolved by electrophoresis and 2′-*O*-methylated RNAs revealed by radiography. (**D**) Efficient methylation requires juxtapositioned RNPs. RNP complexes assembled upon the box C/D and C′/D′ halfmer RNAs were incubated with their respective target RNAs and assayed for methylation. sR8 (D) target RNA (solid square) is the control level of methylation for the box C/D core RNP when positioned in the full-length sR8 sRNP.

To study the structure and function of the box C/D and C′/D′ RNPs independently of each other, sR8 'halfmers' were constructed (Figure 1B and C, upper panels). The C/D RNA contains the 5′/3′ terminal stem, boxes C and D, and the guide sequence upstream of box D. The C′/D′ RNA possesses internal boxes C′ and D′ as well as both guide sequences. The second, box D-associated guide sequence and terminal stem were added to the C′/D′ halfmer to facilitate RNP assembly. Smaller RNAs lacking these added elements assembled little RNP complex, suggesting a perturbed C′/D′ structure (data not shown). RNP assembly for each RNA motif exhibited the same order of protein binding as the complete sR8 sRNA, and the fully assembled RNP III complex contained all three sRNP core proteins (Figure 1B and C, lower panels). Analysis of L7 binding to sR8, C/D and C′/D′ RNAs to form RNP I complexes revealed a predominantly slower migrating complex for full-length sR8 compared with the faster migrating complexes for the C/D and C′/D′ halfmers (compare Figure 1A, B and C, lanes 2 of lower panels). This is consistent with L7 binding both C/D and C′/D′ motifs on the full-length sR8 versus a single L7 protein on each halfmer. Nuclease mapping of L7 binding upon sR8 has demonstrated L7 binding to both motifs (data not shown). Interestingly, subsequent binding of the Nop56/58 and fibrillarin proteins to the C/D and C′/D′ halfmers to assemble RNP complexes II and III is less efficient than that observed for the full-length sR8 RNA, particularly for the terminal box C/D core motif. We suspect that the smaller size of the box C/D RNA with a constrained loop structure likely affects the interaction of Nop56/58 and fibrillarin with the RNA, thus assembling less RNP II and III complexes. These results demonstrate that both archaeal RNP complexes are symmetric with respect to core protein composition and require all three core proteins for RNP assembly.

Nop56/58 and fibrillarin associate through protein–protein interactions and can bind the C′/D′ motif in the absence of L7

The limited binding of Nop56/58 and fibrillarin to sR8 in the absence of L7 (Figure 1A, lane 7) suggested that these two core proteins working together as a complex can bind box C/D sRNAs. Therefore, Nop56/58 and fibrillarin were incubated with the sR8 half-molecules to assess their binding to the box C/D and C′/D′ motifs (Figure 2A). Despite very limited protein binding, these two core proteins interacted with the internal C′/D′ motif but not the terminal box C/D core motif. Competition studies demonstrated the specificity of this interaction, indicating that each motif presents a unique folded structure for protein binding. Although considerably weaker in binding affinity than when assembled in the complete RNP complex, these results clearly demonstrated the ability of Nop56/58 complexed with fibrillarin to bind the C′/D′ motif independently of L7. This observation has implications for the evolution of RNA-binding capabilities of these core proteins and the contrasting organization of the archaeal and eukaryotic box C/D RNPs (see Discussion).

Protein–protein interactions between the sRNP core proteins were explored using *in vitro* 'pulldown' experiments. sRNP core proteins were incubated in pairs, with one of the proteins possessing a His tag, and

coprecipitation of the untagged core protein with its His-tagged partner was assessed by SDS–PAGE (Figure 2B). No interaction between L7 and Nop56/58 or between L7 and fibrillarin was noted. However, interaction between fibrillarin and Nop56/58 was observed, consistent with our belief that these two proteins likely bind the sRNA as a complex. The possibility that Nop56/58 and fibrillarin were interacting via contaminating RNA in the recombinant protein preparations was ruled out by pretreating the proteins with RNase (data not shown). The recently reported cocrystal structure of the *Archaeoglobus fulgidus* Nop56/58–fibrillarin complex (Aittaleb *et al*., 2003) is consistent with our pulldown experiments and supports the idea that these proteins function *in vivo* as a dimer.

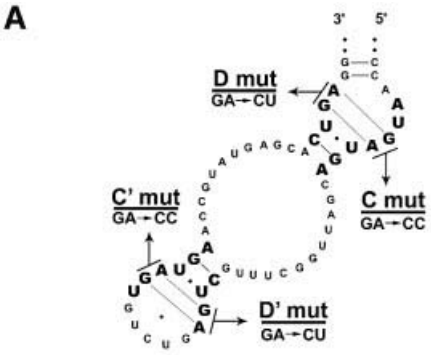

B

Guide RNA	D Target (pmoles in 60 min minus D-CH_3 background (% of wild-type))	D' Target (pmoles in 60 min minus D-CH_3 background (% of wild-type))
sR8 Wild-type	25.6 ± 2.7 (100%)	30.0 ± 0.5 (100%)
C/D RNA	8.7 ± 1.8 (34%)	n. a.
C'/D' RNA	n. a.	-0.8 ± 0.3 (0%)
C/D + C'/D' RNA	10.7 ± 1.2 (42%)	1.0 ± 0.3 (3%)
sR8 C mut	6.3 ± 0.5 (25%)	1.6 ± 0.2 (5%)
sR8 C' mut	0.2 ± 0.2 (0%)	13.6 ± 1.0 (45%)
sR8 D mut	0.4 ± 0.1 (2%)	17.5 ± 1.4 (58%)
sR8 D' Mut	6.9 ± 1.0 (27%)	1.4 ± 0.2 (5%)

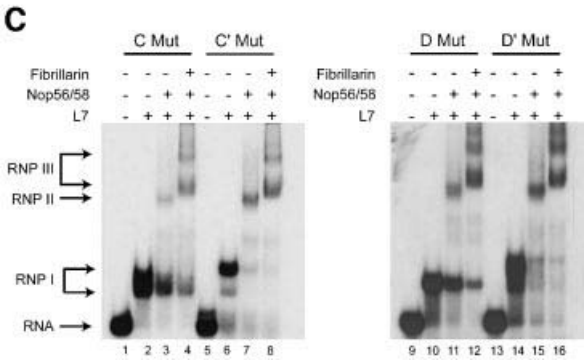

Fig. 4. Mutation of either the terminal box C/D core or internal C′/D′ motifs in full-length sR8 affects guided 2′-*O*-methylation of both RNP complexes. (**A**) Schematic presentation of sR8 sRNA with various mutations in the box C, D, C′ and D′ sequences. For simplicity, the complete terminal helix is not shown but it is present in all mutant sRNAs. (**B**) Box C/D or C′/D′ mutations affect methylation activity of both RNPs. Methylation efficiencies of wild-type sR8, halfmer RNAs and the full-length mutants are reported as total picomoles of methyl incorporation into the target RNAs in 1 h. Methylation of the control D-CH_3 or D′-CH_3 target is subtracted as background. Numbers in parentheses indicate the percentage of methylation with respect to activity of the respective RNPs in the full-length sR8 sRNA. (**C**) RNP complexes are assembled on sR8 box C/D and C′/D′ RNA mutants. sR8 RNAs containing the individual mutants illustrated in (A) were radiolabeled and incubated with the sRNP core proteins as indicated above each gel lane. Assembled complexes were resolved on native polyacrylamide gels and visualized by autoradiography.

The ability of the Nop56/58–fibrillarin complex to bind the C′/D′ motif in the absence of L7 raised the question as to whether L7 is ultimately displaced upon Nop56/58–fibrillarin binding. This possibility was assessed in RNP 'pulldown' experiments using His-tagged fibrillarin for RNP assembly on the RNA halfmers (Figure 2C and D). Co-isolation of the box C/D or C′/D′ RNA using His-tagged fibrillarin required the presence of all three core proteins for efficient RNP assembly. Identical results were obtained for both RNAs, thus demonstrating the symmetry of each RNP complex with respect to core protein content. Of particular note in the control experiments (Figure 2D, lane 8) was the small amount of Nop56/58 co-isolated with His-tagged fibrillarin when L7 was absent. The highly charged character of Nop56/58 in the presence of RNA results in non-specific aggregation and loss of soluble material for gel analysis. This aggregation is not a problem when Nop56/58 and fibrillarin are incubated together in the absence of RNA (Figure 2B). The same aggregation was noted when these two proteins were incubated with RNA for gel shift analysis (Figure 1A). However, the small amounts of radiolabeled RNA used in these experiments minimized these solubility problems. Collectively, these experiments demonstrate the importance of L7 for both box C/D and C′/D′ RNP assembly and the symmetry of the assembled RNP complexes.

The terminal box C/D RNP is the minimal methylation complex but efficient methylation requires that the box C/D and C′/D′ RNPs are juxtaposed in the full-length RNA

The ability of the *in vitro* assembled sR8 sRNP to guide the methylation of RNA substrates was assessed by monitoring the incorporation of [^{3}H]CH_3 donated from *S*-adenosyl-L-methionine (SAM) into substrate RNAs. Target substrates of 21 and 16 nucleotides contained sequences complementary to the terminal box C/D RNP guide sequence (D target) and the internal C′/D′ guide sequence (D′ target), respectively (Figure 3A). Determination of TCA-precipitable counts into the target RNAs revealed that both the terminal box C/D core and internal C′/D′ motifs of the assembled sR8 RNP guided methylation of their target RNAs (Figure 3B). Similar to *in vitro* methylation guided by the *S.acidocaldarius* box C/D sRNP (Omer *et al*., 2002), an elevated temperature of 68°C was required for 2′-*O*-methylation activity (data not shown). Target RNAs possessing a methyl group at the 2′-*O*-ribose position of the designate nucleotide prior to incubation with the assembled sRNP (D-CH_3 and D′-CH_3) (Figure 3A) showed no incorporation of [^{3}H]CH_3. Incubation of both target RNAs in the same methylation reaction correspondingly increased the incorporation of

CH_3 into RNA, and electrophoretic analysis of these substrates demonstrated that CH_3 incorporation was blocked when either substrate was previously methylated at the designate nucleotide (Figure 3C). At present, we do not know whether both RNAs can be methylated by the sRNP simultaneously or if the binding of one substrate precludes binding of the second.

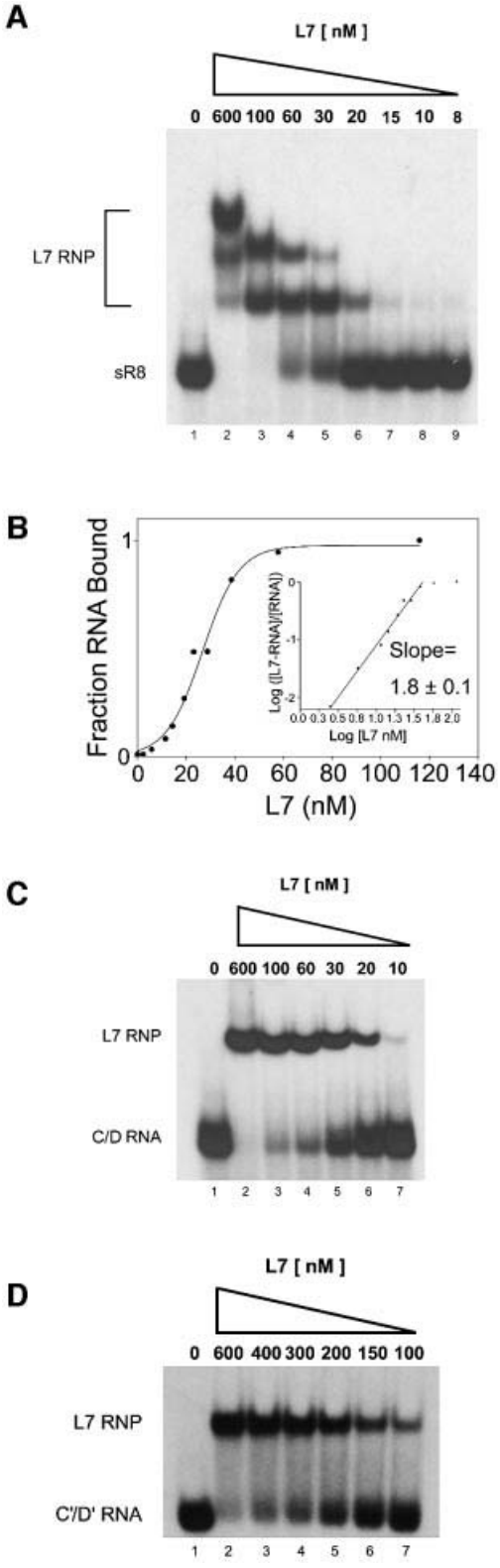

The ability of the terminal box C/D core and internal C′/D′ RNP complexes to guide methylation independently was subsequently examined. Strikingly, guided methylation from each assembled half-molecule RNP was adversely affected (Figure 3D). The level of 2′-*O*-methylation for the terminal box C/D RNP complex was reduced to approximately one-third of that observed for this complex in full-length sR8, while the assembled C′/D′ RNP was completely inactive. Incubation of the two RNP complexes together *in trans* did not restore the methylation activity of either RNP (Figure 4B). These results revealed two important catalytic features of the archaeal box C/D sRNP complex. First, the minimal RNP structure capable of directing nucleotide-specific 2′-*O*-methylation, albeit at reduced levels, is the terminal box C/D RNP. Secondly, maximal methylation efficiency of both the box C/D and C′/D′ RNP complexes requires that they be juxtapositioned within the full-length sRNA molecule.

Mutations in conserved box elements impair methylation from both guide regions

The importance of positioning the two RNP complexes within the full-length sRNA for optimal methylation activity was further examined in sR8 mutagenesis experiments. Mutations were made in the critical GA dinucleotides of each box element (Figure 4A). Each mutant sRNA assembled with sRNP core proteins was assayed for methylation activity guided from both motifs (Figure 4B). Mutation of box C reduced methylation of the D target as expected, but also severely disrupted methylation of the D′ target. Similarly, mutation of the C′ sequence affected methylation from both mutated and non-mutated motifs. Mutations in box D and D′ sequences also affected methylation of both target RNAs, but resulted in greater inhibition of methylation guided by the mutated C/D or C′/D′ motifs. These results confirmed the critical nature of positioning box C/D and C′/D′ RNPs within the full-length sRNA for obtaining efficient methylation activity.

The effect of the box C/D and C′/D′ mutations upon sRNP assembly was examined to determine whether the loss of methylation activity in the non-mutated motif was due to lack of RNP assembly (Figure 4C). Mutant C, D, C′ and D′ sR8 sRNAs were incubated with the core proteins and assembled RNP complexes resolved on polyacrylamide gels. All four mutant sRNAs bound all three sRNP core proteins and assembled higher-order

Fig. 5. Core protein L7 exhibits cooperative binding to archaeal sR8 sRNA. (**A**) L7 protein binds the box C/D and C′/D′ motifs of sR8 sRNA. Increasing concentrations of L7 were incubated with radiolabeled sR8. Assembled RNP complexes were resolved on native polyacrylamide gels and visualized by autoradiography. The slowest migrating L7 RNP (lane 2) is observed only at excess L7 concentrations and represents non-specific L7 binding. (**B**) L7 association with the sR8 box C/D and C′/D′ motifs is cooperative. Increasing concentrations of L7 were incubated with radiolabeled sR8, assembled RNP complex blotted to nitrocellulose membranes and assembled RNP quantified using a PhosphorImager. The fraction of RNA bound in the RNP complex is plotted as a function of L7 concentration. L7 binding data are also presented as a Hill plot (inset). (**C** and **D**) L7 binds to both the terminal box C/D core and internal C′/D′ halfmer RNAs. Increasing concentrations of L7 were incubated with radiolabeled terminal box C/D (C) or internal C′/D′ halfmers (D). Assembled RNP complexes were resolved on native polyacrylamide gels and visualized by autoradiography.

RNP III complexes. Interestingly, closer inspection of RNP assembly indicated differences in complex formation when the terminal box C/D core motif was mutated as opposed to the internal C′/D′ motif. Binding of L7 to the box C or D mutants resulted in a faster migrating RNP I complex as compared with the C′ and D′ mutants (Figure 4C). The different migration of these RNP I complexes indicated that L7 is primarily binding the C′/D′ motif. However, some methylation is still guided by the box C/D core RNP, particularly with the box C mutant, suggesting limited L7 binding and RNP assembly on the C/D motif. In contrast, the C′ and D′ mutant sRNAs

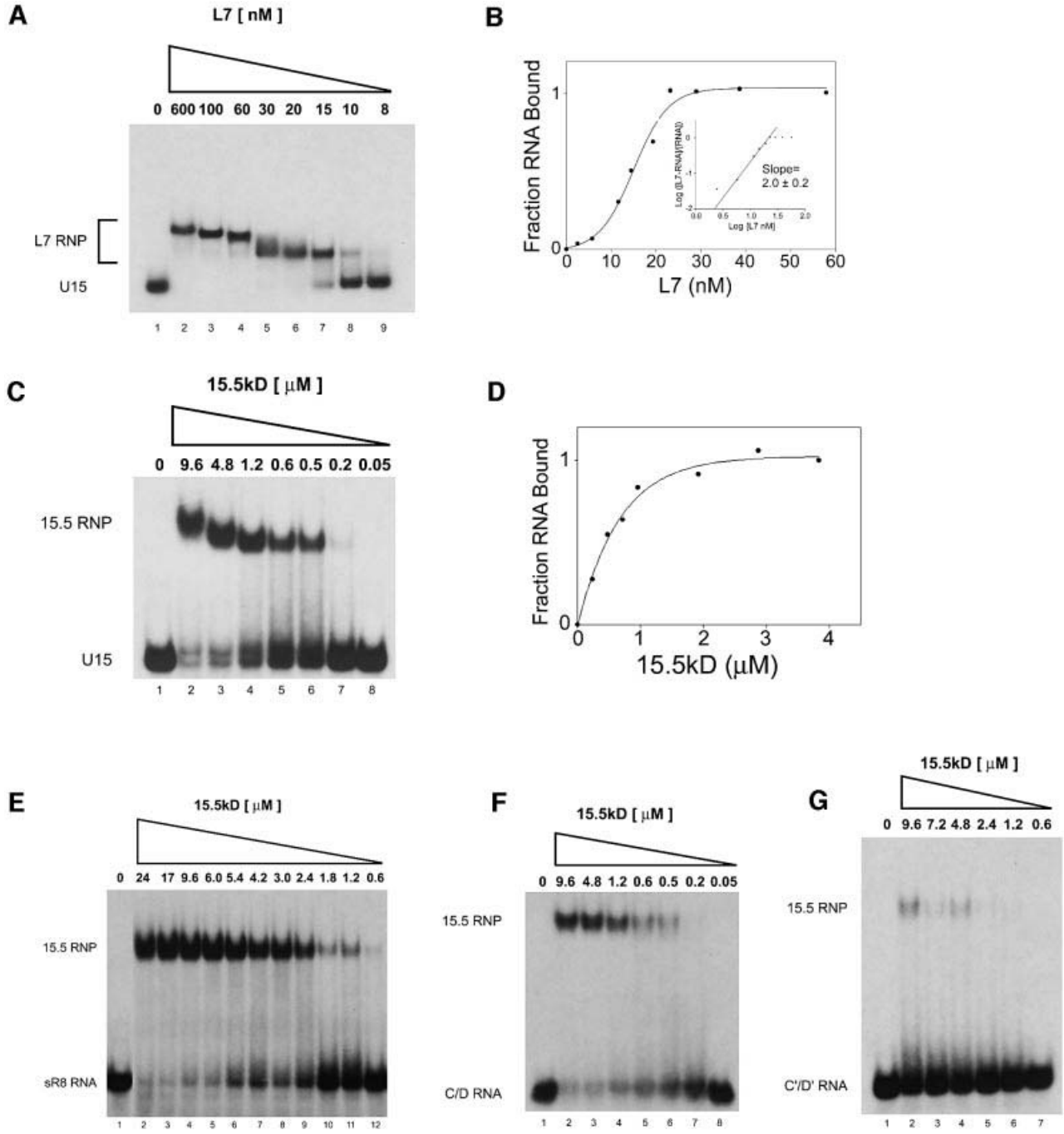

Fig. 6. Archaeal L7 binds both the C/D and C′/D′ motifs, while eukaryotic 15.5 kDa protein binds only the terminal box C/D core motif. (**A**) Increasing amounts of *M.jannaschii* L7 protein were incubated with radiolabeled human U15 snoRNA. Assembled RNP complexes were resolved on a native polyacrylamide gel and visualized by autoradiography. (**B**) Archaeal sRNP core protein L7 exhibits cooperativity in binding to U15 snoRNA. Binding analyses were performed as detailed in Figure 5. (**C**) Eukaryotic snoRNP core protein 15.5 kDa binds only the U15 box C/D core motif. Increasing amounts of mouse 15.5 kDa protein were incubated with radiolabeled human U15 snoRNA. Assembled RNP complexes were resolved on a native polyacrylamide gel and visualized by radiography. (**D**) The fraction of U15 snoRNA bound in an RNP complex is plotted as a function of 15.5 kDa concentration. Increasing amounts of mouse 15.5 kDa core protein were incubated with radiolabeled full-length archaeal sR8 sRNA (**E**) and halfmer RNAs possessing either the terminal box C/D (**F**) or internal C′/D′ (**G**) motifs. Assembled RNP complexes were resolved on native polyacrylamide gels and visualized by radiography.

apparently bind two L7 proteins, as evidenced by slower migrating RNP I complexes, and this has been confirmed with L7 titration experiments (data not shown). Despite L7 binding at both RNA motifs and subsequent RNP assembly which mirrors formation of the wild-type RNP complex (Figure 1), methylation is adversely affected at both the mutated C′/D′ and non-mutated C/D motifs. Therefore, observed loss of methylation activity at the non-mutated motif is a consequence of crosstalk between the two RNP complexes and not a failure to assemble an RNP complex.

Archaeal L7 binds cooperatively to the box C/D and C′/D′ motifs

The importance of juxtaposed RNPs in guided methylation prompted us to examine the possible cooperative nature of box C/D and C′/D′ RNP assembly. Since L7 binding initiates sRNP assembly, the nature of its binding to the two RNA motifs was examined. Titration of sR8 with increasing concentrations of L7 revealed the formation of two RNP complexes (Figure 5A). Footprinting analysis has demonstrated L7 binding to both C/D and C′/D′ motifs (data not shown). The slowest migrating RNP in lane 2 is seen with excess concentrations of protein and results from non-specific binding of L7 to RNA. The strength and cooperative nature of L7 binding to sR8 were demonstrated in filter-binding experiments where L7 binding revealed a sigmoidal binding curve, indicative of cooperative binding (Figure 5B). Hill plot analysis confirmed the cooperative nature of L7 interaction with a determined slope of 1.8 (slopes >1 indicate positive cooperativity). Dissociation constants (K_d) of 9 and 19 nM were calculated. At this time, we are not able to correlate each K_d value with L7 recognition of a specific RNA motif.

L7 bound both sR8 half-molecules (Figure 5C and D) with K_d values of 10 and 54 nM for the box C/D and C′/D′ motifs, respectively. Interestingly, the L7 binding affinities to the two motifs relative to each other were affected when the motifs were no longer positioned in full-length sR8 sRNA. A significant increase in one K_d was noted (9 and 19 nM versus 10 and 54 nM) when the two motifs bound L7 independently. This is consistent with the observed positive cooperativity of L7 binding to full-length sR8 sRNA.

Archaeal L7 and eukaryotic 15.5 kDa core protein homologs exhibit different RNA recognition specificities for box C/D and C′/D′ RNA binding

The archaeal box C/D sRNP complex exhibits a symmetric core protein distribution with L7 binding both the box C/D and C′/D′ motifs. This is in contrast to the asymmetric eukaryotic snoRNP where the 15.5 kDa protein binds only the terminal box C/D core motif (Cahill *et al*., 2002; Szewczak *et al*., 2002). To compare RNA recognition specificities of the archaeal and eukaryotic homologs of this core protein, the binding of archaeal L7 to eukaryotic U15 snoRNA was examined first. Strikingly, like its binding to archaeal sR8, L7 bound both the box C/D and C′/D′ motifs of U15 snoRNA (Figure 6A). Binding analysis revealed a sigmoidal curve with calculated K_d values of 5 and 8 nM, and Hill plot analysis was consistent with the cooperative nature of L7 binding (Figure 6B). The binding of 15.5 kDa protein, the eukaryotic homolog of archaeal L7, was assessed next for its interactions with eukaryotic and archaeal box C/D RNAs. As previously reported (Szewczak *et al*., 2002), 15.5 kDa protein bound only the U15 snoRNA box C/D motif (Figure 6C). Consistent with single-site binding, the 15.5 kDa binding curve was not sigmoidal (Figure 6D). Similarly, 15.5 kDa protein bound only the terminal box C/D core motif of archaeal sR8 sRNA (Figure 6E, F and G). Collectively, these binding studies demonstrated the different RNA recognition specificities of the L7 and 15.5 kDa core protein homologs. These differences in RNA-binding capabilities thus provide a biochemical rationale for the different distribution of this protein in the archaeal versus eukaryotic box C/D RNPs.

Discussion

Assembly of the terminal box C/D core and internal C′/D′ RNP complexes requires the ordered addition of the sRNP core proteins and elevated temperatures, as previously observed for an *S.acidocaldarius* box C/D sRNP complex (Omer *et al*., 2002). Reconstitution experiments demonstrated that Nop56/58 associates with the sRNA following L7 binding and is then joined by fibrillarin (Omer *et al*., 2002; this study). However, it is clear that Nop56/58 binding is enhanced in the presence of fibrillarin and that Nop56/58 and fibrillarin can bind the C′/D′ motif in the absence of L7. We believe that these two core proteins likely associate prior to RNA binding. Our pulldown experiments demonstrating interaction between these two core proteins is consistent with this idea. The recent cocrystal structure of this protein complex also supports this idea with the demonstration of heterodimer formation in the absence of sRNA substrate (Aittaleb *et al*., 2003).

Our assembly experiments have established the symmetric organization of the archaeal sRNP complex with all three core proteins binding the box C/D and C′/D′ motifs. This is of particular importance in light of recent investigations of the eukaryotic snoRNP complex revealing an asymmetric distribution of core proteins upon the two RNA motifs. In contrast with eukaryotic 15.5 kDa protein, which binds exclusively to the box C/D core motif, archaeal L7 also binds the C′/D′ RNA. Omer *et al*. (2002) previously observed multiple RNPs upon L7 binding to an *S.acidocaldarius* box C/D sRNA but suggested that they were conformational isomers of the L7:RNA complex. We have now demonstrated L7 binding to both motifs. As demonstrated in RNP pulldown analysis, L7 is necessary for assembly of both the box C/D and C′/D′ RNP complexes. L7 clearly binds these two motifs in a cooperative manner. Although the exact nature of this cooperativity is not known, it could reflect induced changes in sR8 structure following initial L7 binding and/or protein–protein interactions between the two L7 molecules. Interestingly, the crystal structure of the Nop56/58–fibrillarin heterotetramer has suggested that the Nop56/58 proteins of box C/D and C′/D′ RNPs might also interact via protein–protein interactions. Thus the requirement that efficient methylation of both complexes requires their juxtaposition on the same sRNA may reflect multiple protein–protein interactions between the two RNPs.

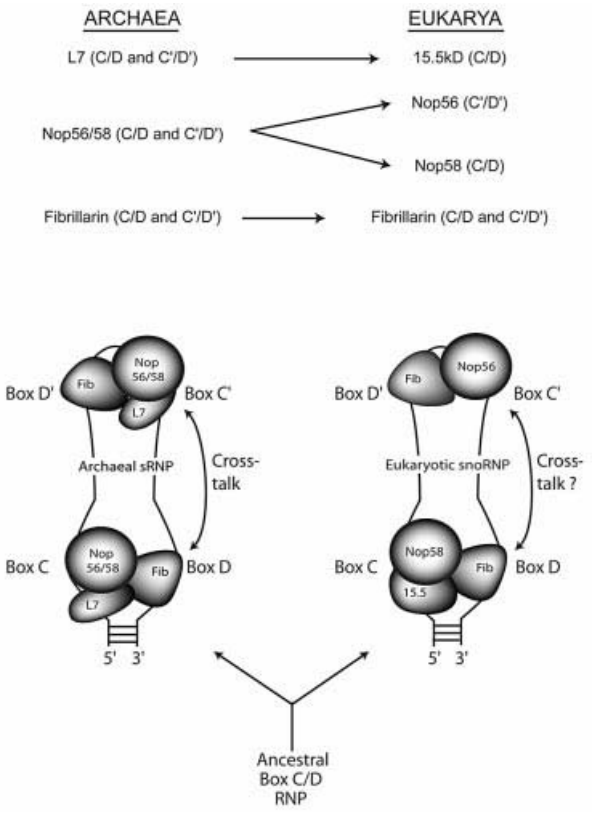

Fig. 7. Archaeal and eukaryotic box C/D RNP complexes exhibit symmetric versus asymmetric distribution of the RNP core proteins bound to sRNAs and snoRNAs, respectively. The illustrated structure of the eukaryotic snoRNP is based on the work of Cahill *et al*. (2002) and Szewczak *et al*. (2002).

Strikingly, differential binding of Nop56/58 and fibrillarin to the C/D and C′/D′ halfmers demonstrates the structural distinctness of the two RNA motifs. The C′ and D′ sequences are well conserved in Archaea but less so in Eukarya, and are often hard to identify in the snoRNAs (Kiss-Laszlo *et al*., 1998; Omer *et al*., 2000). Of particular note is the lack of strict conservation of the GA nucleotides of the eukaryotic C′/D′ motif, which are crucial for establishing the K-turn structure (Klein *et al*., 2001; Kuhn *et al*., 2002). This suggests that the C′/D′ motif does not adopt a canonical kink-turn structure. Observations by other workers (Cahill *et al*., 2002) have also shown that the GA nucleotides of box D′ are not required for snoRNA-guided methylation from the C′/D′ RNP. Thus available evidence now suggests that the C′/D′ motif is, at least, a variation of the classical K-turn fold exhibited by the box C/D motif.

Unexpectedly, methylation activity of the sR8 half-molecules was severely reduced or abolished when the two RNP complexes were no longer juxtaposed within the full-length sRNA. It is not yet clear how each RNP complex affects the methylation activity of the other. It is possible that binding of core proteins at one motif affects the folded RNA structure at the second motif and/or involves protein–protein interactions between the two RNP complexes. However, the ability of both motifs to assemble complete RNP complexes with halfmer RNAs demonstrates that complete RNP assembly on each can proceed in the absence of the other. Interestingly, mutations in boxes C and C′ of full-length sR8 affected the activity of the non-mutated motif more significantly than that of the mutated motif. In contrast, the box D and D′ mutants had the most severe effect upon the methylation activity of the mutated motif. These observations suggest that the two nucleotide sequence elements contribute differently to methylation activity, possibly through core protein binding. This is consistent with the protein–RNA crosslinking results (Cahill *et al*., 2002) which revealed that different core proteins associate with each box sequence element.

At present, it is not known whether juxtapositioning the terminal box C/D and internal C′/D′ motifs in eukaryotic snoRNAs is also important for efficient methylation activities. However, two lines of evidence suggest that protein–protein interactions may occur between the core proteins of the box C/D and C′/D′ RNPs. In characterizing U14 snoRNP proteins, we isolated Nop56 as well as Nop58 using a minimal terminal box C/D core motif for affinity purification (Newman *et al*., 2000). Since the core proteins of the eukaryotic snoRNP complex are asymmetrically distributed with Nop56 bound only to the internal C′/D′ motif, this suggests that the co-isolation of Nop56 with Nop58 may be the result of protein–protein interactions. Secondly, it has been shown (Watkins *et al*., 2002) that mutations within box C/D stem II affect the binding of both Nop56 and Nop58. The loss of both proteins upon alteration of only one motif again suggests protein crosstalk between the two RNPs.

Comparison of the archaeal and eukaryotic box C/D RNPs reveals structurally distinct complexes (Figure 7). The eukaryotic snoRNP is comprised of four core proteins compared with three for the archaeal sRNP. A duplication event has resulted in the two Nop56/58 genes found in eukaryotes with each coding sequence evolving to produce proteins with different snoRNA-binding capacities (Dennis *et al*., 2001). Interestingly, the primary sequence of archaeal Nop56/58 displays equal homology with eukaryotic Nop56 and Nop58 (data not shown). The ability of archaeal Nop56/58 and fibrillarin to weakly but specifically recognize the C′/D′ motif in the absence of L7 is strikingly similar to eukaryotes. In Archaea, L7 contributes to Nop56/58–fibrillarin binding and has been retained in the C′/D′ RNP complex. In contrast, eukaryotic Nop56 has apparently evolved such that 15.5 kDa is no longer necessary for Nop56–fibrillarin binding on the C′/D′ motif. The inability of 15.5 kDa to bind the C′/D′ motif indicates that this core protein is distinctly different from its archaeal homolog in RNA recognition specificity. This is surprising since crystal structures of 15.5 kDa and L7 are virtually superimposable (Kuhn *et al*., 2002). The 15.5 kDa protein has apparently adapted its binding site to the terminal box C/D core motif. The structural basis for their different binding capabilities awaits fine-structure analysis of their interactions with the box C/D motif. In the absence of 15.5 kDa, the structure of the C′/D′ motif has probably drifted from the canonical K-turn to accommodate the Nop56–fibrillarin complex. This could explain the stricter conservation of C′/D′ sequences in Archaea.

Archaeal and eukaryotic box C/D RNAs assemble distinctly different RNPs despite using homologous proteins for RNP construction. The simple and symmetric

archaeal complex has evolved in eukaryotes to a more complex and asymmetric particle. Strikingly, this progression from simple and symmetric to complex and asymmetric may reflect a general evolutionary progression of RNA processing/modification systems that are shared by both Archaea and Eukarya (Li *et al*., 1998). The tRNA splicing machinery of *M.jannaschii* is a tetramer composed of four identical subunits that recognize the two splice sites and carry out both endonuclease and ligase functions. This same processing complex in eukaryotes is again a tetramer but composed of four different proteins. Despite their homology with the archaeal proteins, the eukaryotic subunits have evolved specialized functions and even exhibit a different mechanism for splice site recognition. Analysis of eukaryotic snoRNAs suggests that at least some box C/D RNAs have also undergone a specialization of RNP function. U14 is such an snoRNA where the terminal box C/D RNP guides methylation of 18S rRNA and the internal C′/D′ element functions as an RNA chaperone to direct pre-rRNA cleavage and processing. The recent observation that the methylation and chaperone functions of *Drosophila melanogaster* U14 are contained on two different snoRNA species suggests that RNP specialization may have progressed further in Diptera (Yuan *et al*., 2003). Determination of possible differences in RNP organization reflecting the observed increase in complexity of snoRNA function awaits further investigation.

Materials and methods

DNA template construction and RNA synthesis

Target RNA substrates and the box C/D sR8 half-molecule were purchased from Dharmacon Research Inc. Sequences are reported in the 5′ to 3′ direction and the 2′-*O*-methylated nucleotide is designated with an 'm' preceding the modified nucleotide. Box C/D RNA halfmer: AAAUCGCCAAUGAUGAAACGUAUGAGCACUGAGGCGAUUU; D target: CUGAUGCUCAUACGGUCUGCU; D′ target: GCUCAAAGCCAAUCGC; D-CH_3: CUGAUGCUmCAUACGGUCUGCU; D′-CH_3: GCUCAAAmGCCAAUCGC.

Longer RNAs were synthesized by *in vitro* transcription using DNA templates. Full-length sR8 DNA was amplified from *M.jannaschii* genomic DNA and mutant sR8 templates were generated by PCR amplification from this full-length DNA template. Human U15A snoRNA template was amplified from plasmid pBS-U15 (Watkins *et al*., 1996). RNA transcripts were synthesized using the RiboMAX Large Scale RNA Production System-T7 (Promega) according to the manufacturer's protocol. RNAs were gel purified and 5′ labeled with T4 polynucleotide kinase and [γ-^{32}P]ATP.

PCR primer pairs for amplification of DNA templates

Wild-type sR8 DNA template (1+2); C mut (2+3); C′ mut (1+4); D mut (1+5); D′ mut (1+6); C′/D′ RNA halfmer (7+8); U15 (9+10). (1) CTAATACGACTCACTATAGGCCAAATCGCCAATGATGACGATTG; (2) AAATCGCCTCAGTGCTCATACGG; (3) CTAATACGACTCACTATAGGCCAAATCGCCAATCCTGACGATTG; (4) AAATCGCCTCAGTGCTCATACGGTTCAGGACAGAC; (5) AAATCGCCAGAGTGCTCATACGG; (6) AAATCGCCTCAGTGCTCATACGGTTCATCACAGACAGAGC; (7) CTAATACGACTCACTATAGGCCTCTGGCGATTGGCTTTGCTGAGTC; (8) TCTGGAGTGCTCATACGGTTCATC; (9) CTAATACGACTCACTATAGGCCCTTCGATGAAGAGATGATGACG; (10) CCTTCTCAGACAAATGCCTCTAAG.

Cloning, expression and purification of proteins

Recombinant GST-tagged mouse 15.5 kDa protein was expressed and purified as previously described (Kuhn *et al*., 2002). Genes encoding L7, Nop56/58 and fibrillarin proteins were amplified from *M.jannaschii* genomic DNA using primer pairs which placed restriction sites on the 5′ and 3′ sides of the template (*Nde*I/*Bam*HI for L7 and fibrillarin, and *Nco*I/*Bam*HI for Nop56/58) for subsequent cloning. Following restriction digestion, protein-coding templates were ligated into a pET28a vector (Novagen) resulting in N-terminally His-tagged L7 and fibrillarin, and untagged Nop56/58. Proteins were expressed in Rosetta (DE3) cells (Novagen) at 37°C for 3 h (L7 and fibrillarin) or at 15°C overnight (Nop56/58). His-tagged proteins were purified by nickel-affinity chromatography using 'His-bind' Resin (Novagen) according to the manufacturer's protocol. Affinity tags were removed with thrombin cleavage overnight at 4°C. Nop56/58 was purified (to ~80% homogeneity) by cation exchange chromatography using SP-Sepharose Fast-Flow Resin (Sigma) and bound protein eluted with an NaCl gradient. Isolated archaeal proteins were dialyzed against buffer D (20 mM HEPES pH 7, 100 mM NaCl, 3 mM $MgCl_2$, 0.2 mM EDTA, 20% glycerol) at 4°C overnight.

Protein–RNA interactions analyzed by EMSA and filter binding

RNP complexes were assembled under the following conditions. Radiolabeled RNA (0.2 pmol) was incubated with increasing concentrations of L7 or GST-tagged 15.5 kDa for binding analysis. L7 RNP complex formation was assessed by titrating L7 (8–600 nM) in 20 µl reactions supplemented with 10 µg of tRNA in binding reaction buffer (20 mM HEPES pH 7, 150 mM NaCl, 0.75 mM dithiothreitol, 1.5 mM $MgCl_2$, 0.1 mM EDTA, 10% glycerol). Complexes were assembled by incubation at 70°C for 10 min. GST–15.5 kDa complexes were assembled at 30°C for 30 min under the same binding conditions with increasing protein concentrations from 0.6 to 24 µM. Formation of higher-order archaeal RNP complexes included 10 pmol of L7, 32 pmol of Nop56/58 and 33 pmol of fibrillarin added either individually or in different combinations. Complexes were resolved by electrophoretic mobility-shift analysis (EMSA) on 4 or 6% phosphate-buffered polyacrylamide gels pH 7 containing 2% glycerol and RNPs were visualized by autoradiography. RNP complexes for competition analysis were assembled under the same conditions as above but with 64 pmol of Nop56/58 and no L7. Unlabeled competitor RNAs (C/D or C′/D′ RNA halfmers) were added at 1000-fold molar excess and RNP complexes were resolved by native gel electrophoresis. L7 and 15.5 kDa binding affinity with sR8 and U15 was assessed using a nitrocellulose filter-binding assay. Binding conditions were the same as for EMSA with the following modifications: 50 µl reactions were assembled with 0.1 nM radiolabeled RNA and L7 (2.5–58 nM) or 15.5 kDa (0–4 µM). Samples were applied to a nylon membrane using a dot-blot apparatus, washed and dried. Bound radioactivity was visualized using a Molecular Dynamics Model 425F PhosphorImager and quantified using the ImageQuant v3.3 software package. Calculations of dissociation constants and cooperativity measurements were performed using the Prism v3.00 software package (GraphPad).

Protein–protein interactions analyzed by in vitro co-selection

Box C/D sRNP core proteins were incubated at equimolar concentrations in buffer A (20 mM HEPES, 100 mM NaCl, 1 mM $MgCl_2$) for 30 min at 23°C. Then, 20% of the protein mixture was removed and designated applied sample, while the remainder was incubated with 15 µl of 'His-bind' resin (Novagen). Protein-bound resin was washed six times with buffer A supplemented with 60 mM imidazole, 0.1% Triton X-100 and 0.025% SDS. Bound proteins were eluted with buffer A containing 1 M imidazole. Applied and eluted protein samples were resolved on 14% SDS–polyacrylamide gels and visualized by Coomassie Blue staining. Selected protein samples were treated for 1 h at 23°C with 0.064 and 32 U of RNases A and T1, respectively, prior to affinity selection on His-bind resin. RNP pulldown experiments were accomplished by assembling C/D and C′/D′ RNP complexes in binding buffer minus EDTA and at RNA concentrations of 90 ng/µl. RNP complex selection was accomplished using His-tagged fibrillarin and His-bind resin as detailed above. Portions of the RNP eluates were phenol extracted, ethanol precipitated and RNA analyzed on 10% polyacrylamide–7 M urea gels.

In vitro methylation

sRNP complexes were assembled as described for EMSA analysis but in 80 µl reaction volumes containing 52 pmol of RNA. Assembled RNP complexes were mixed with 720 pmol of anti-sense target RNA, 360 pmol of SAM (*S*-adenosyl-L-methionine dihydrogen sulfate; Calbiochem) and 1.6 µCi of [^{3}H]SAM (55 Ci/mmol; ICN Biomedicals) in a final reaction volume of 120 µl in binding reaction buffer. Reactions were incubated at 68°C and 20 µl aliquots removed at 0, 10, 20, 40 and 60 min for TCA precipitation. Aliquots were spotted onto Whatman 3MM filters, dried, precipitated onto filters with 10% TCA for 15 min at 4°C and then washed

three times with 5% TCA at 23°C for 1 h. Filters were dried and [^{3}H]CH_3 incorporation determined by scintillation counting. Assays performed in triplicate consistently revealed small mean deviations of determined counts. Methylated RNA targets were also phenol extracted, ethanol precipitated, resolved on 12% polyacrylamide–7 M urea gels and visualized by radiography using BioMax intensifying screens and film (Kodak).

Acknowledgements

We thank Maurille Fournier and Ramesh Gupta for critical reading of the manuscript and James Brown for providing *M.jannaschii* genomic DNA. Initial stages of this work were supported by NSF Grant MCB 9727945 (E.S.M.).

References

Aittaleb,M., Rashid,R., Chen,Q., Palmer,J., Daniels,C. and Li,H. (2003) Structure and function of archaeal box C/D sRNP core proteins. *Nat. Struct. Biol.* **10**, 256–263.

Amiri,K. (1994) Fibrillarin-like proteins occur in the domain Archaea. *J. Bacteriol*., **176**, 2124–2127.

Bachellerie,J.P., Cavaille,J. and Huttenhofer,A. (2002) The expanding snoRNA world. *Biochimie*, **84**, 775–790.

Caffarelli,E., Fatica,A., Prislei,S., DeGregorio,E., Fragapane,P. and Bozzoni,I. (1996) Processing of the intron-encoded U16 and U18 snoRNAs: the conserved C and D boxes control both the processing reaction and the stability of the mature snoRNA. *EMBO J.*, **15**, 1121–1131.

Cahill,N., Friend,K., Speckman,W., Li,Z., Terns,R., Terns,M. and Steitz,J. (2002) Site-specific cross-linking analyses reveal an asymmetric distribution for a box C/D snoRNP. *EMBO J.*, **21**, 3816–3828.

Cavaille,J. and Bachellerie,J.P. (1996) Processing of fibrillarin-associated snoRNAs from pre-mRNA introns: an exonucleolytic process exclusively directed by the common stem-box terminal structure. *Biochimie*, **78**, 443–456.

Cavaille,J. and Bachellerie,J.P. (1998) SnoRNA-guided ribose methylation of rRNA: structural features of the guide RNA duplex influencing the extent of the reaction. *Nucleic Acids Res.*, **26**, 1576–1587.

Dennis,P., Omer,A. and Lowe,T. (2001) A guided tour: small RNA function in Archaea. *Mol. Microbiol.*, **40**, 509–519.

Galardi,S., Fatica,A., Bachi,A., Scaloni,A., Presutti,C. and Bozzoni,I. (2002) Purified box C/D snoRNPs are able to reproduce site-specific 2′-*O*-methylation of target RNA *in vitro*. *Mol. Cell. Biol.*, **22**, 6663–6668.

Gaspin,C., Cavaille,J., Erauso,G. and Bachellerie,J.-P. (2000) Archaeal homologs of eukaryotic methylation guide small nucleolar RNAs: lessons from the *Pyrococcus* genomes. *J. Mol. Biol.*, **297**, 895–906.

Jady,B. and Kiss,T. (2001) A small nucleolar guide RNA functions both in 2′-*O*-ribose methylation and pseudouridylation of the U5 spliceosomal RNA. *EMBO J.*, **20**, 541–551.

Kiss,T. (2002) Small nucleolar RNAs: an abundant group of non-coding RNAs with diverse cellular functions. *Cell*, **109**, 145–148.

Kiss-Laszlo,Z., Henry,Y. and Kiss,T. (1998) Sequence and structural elements of methylation guide snoRNAs essential for site-specific ribose methylation of pre-rRNA. *EMBO J.*, **17**, 797–807.

Klein,D., Schmeing,T., Moore,P. and Steitz,T. (2001) The kink-turn: a new RNA secondary structure motif. *EMBO J.*, **20**, 4214–4221.

Kuhn,J., Tran,E. and Maxwell,E.S. (2002) Archaeal ribosomal protein L7 is a functional homolog of the eukaryotic 15.5kD/Snu13p snoRNP core protein. *Nucleic Acids Res.*, **30**, 931–941.

Lafontaine,D. and Tollervey,D. (1999) Nop58p is a common component of the box C+D snoRNPs that is required for snoRNA stability. *RNA*, **5**, 455–467.

Lafontaine,D. and Tollervey,D. (2000) Synthesis and assembly of the box C+D small nucleolar RNPs. *Mol. Cell. Biol.*, **20**, 2650–2659.

Li,H., Trotta,C. and Abelson,J. (1998) Crystal structure and evolution of a transfer RNA splicing enzyme. *Science*, **280**, 279–284.

Newman,D., Kuhn,J., Shanab,G. and Maxwell,S. (2000) Box C/D snoRNA-associated proteins: two pairs of evolutionarily ancient proteins and possible links to replication and transcription. *RNA*, **6**, 861–879.

Omer,A., Lowe,T., Russell,A., Ebhardt,H., Eddy,S. and Dennis,P. (2000) Homologs of small nucleolar RNAs in Archaea. *Science*, **288**, 517–522.

Omer,A., Ziesche,S., Ebhardt,H. and Dennis,P. (2002) *In vitro* reconstitution and activity of a C/D box methylation guide ribonucleoprotein complex. *Proc. Natl Acad. Sci. USA*, **99**, 5289–5294.

Szewczak,L.W., DeGregorio,S., Strobel,S. and Steitz,J. (2002) Exclusive interaction of the 15.5 kD protein with the terminal box C/D motif of a methylation guide snoRNP. *Chem. Biol.*, **9**, 1095–1107.

Tang,T. *et al*. (2002) RNomics in Archaea reveals a further link between splicing of archaeal introns and rRNA processing. *Nucleic Acids Res.*, **30**, 921–930.

Terns,M. and Terns,R. (2002) Small nucleolar RNAs: versatile *trans*-acting molecules of ancient evolutionary origin. *Gene Expr.*, **10**, 17–39.

Tollervey,D. (1996) Small nucleolar RNAs guide ribosomal RNA methylation. *Science*, **273**, 1056–1057.

Tollervey,D., Lehtonen,H., Jansen,R., Kern,H. and Hurt,E.C. (1993) Temperature-sensitive mutations demonstrate roles for yeast fibrillarin in pre-rRNA processing, pre-rRNA methylation and ribosome assembly. *Cell*, **72**, 443–457.

Tyc,K. and Steitz,J. (1989) U3, U8 and U13 comprise a new class of mammalian snRNPs localized in the cell nucleolus. *EMBO J.*, **8**, 3113–3119.

Tycowski,K., You,Z., Graham,P. and Steitz,J. (1998) Modification of U6 spliceosomal RNA is guided by other small RNAs. *Mol. Cell*, **2**, 629–638.

Vidovic,I., Nottrott,S., Hartmuth,K., Luhrmann,R. and Ficner,R. (2000) Crystal structure of the spliceosomal 15.5 kD protein bound to a U4 snRNA fragment. *Mol. Cell*, **6**, 1331–1342.

Wang,H., Boisvert,D., Kim,K., Kim,R. and Kim,S.H. (2000) Crystal structure of a fibrillarin homologue from *Methanococcus jannaschii*, a hyperthermophile, at 1.6 A resolution. *EMBO J.*, **19**, 317–323.

Watkins,N., Leverette,R., Xia,L. Andrews,M. and Maxwell,S. (1996) Elements essential for processing intronic U14 snoRNA are located at the termini of the mature snoRNA sequence and include conserved nucleotide boxes C and D. *RNA*, **2**, 118–133.

Watkins,N. *et al*. (2000) A common core RNP structure shared between the small nucleolar box C/D RNPs and the spliceosomal U4 snRNP. *Cell*, **103**, 457–466.

Watkins,N., Dickmanns,A. and Luhrmann,R. (2002) Conserved stem II of the box C/D motif is essential for nucleolar localization and is required, along with the 15.5 K protein, for the hierarchical assembly of the box C/D snoRNP. *Mol. Cell. Biol.*, **22**, 8342–8352.

Yuan,G., Klambt,C., Bachellerie,J.P., Brosius,J. and Huttenhofer,A. (2003) RNomics in *Drosophila melanogaster*: identification of 66 candidates for novel non-messenger RNAs. *Nucleic Acids Res.*, **31**, 2495–2507.

Received January 27, 2003; revised May 21, 2003; accepted June 2, 2003